UNIVERSIDADE DE SÃO PAULO
FACULDADE DE ODONTOLOGIA DE BAURU

PEDRO RODRIGUES MINIM

Effects of the sintering parameters and the addition of agglutinants on the structural characteristics of bovine hydroxyapatite dense bioceramics

Efeitos dos parâmetros de sinterização e da adição de aglutinantes nas características estruturais de biocerâmicas densas de hidroxiapatita bovina

BAURU
2022

PEDRO RODRIGUES MINIM

Effects of the sintering parameters and the addition of agglutinant agents on the structural characteristics of bovine hydroxyapatite dense bioceramics

Efeitos dos parâmetros de sinterização e da adição de aglutinantes nas características estruturais de Biocerâmicas densas de Hidroxiapatita Bovina

Dissertação constituída por artigo apresentada à Faculdade de Odontologia de Bauru da Universidade de São Paulo para obtenção do título de Mestre em Ciências no Programa de Ciências Odontológicas Aplicadas, na área de concentração Reabilitação Oral.

Orientador: Prof. Dr. José Henrique Rubo

Versão Corrigida

BAURU
2022

Minim, Pedro Rodrigues

Effects of the sintering parameters and the addition of agglutinant agents on the structural characteristics of bovine hydroxyapatite dense bioceramics / Pedro Rodrigues Minim. -- Bauru, 2022/ Pedro Rodrigues Minim. -- Bauru, 2022.
057 p. : il. ; 31 cm.

Dissertação (mestrado) -- Faculdade de Odontologia de Bauru, Universidade de São Paulo, ano de defesa.

Universidade de São Paulo
Faculdade de Odontologia de Bauru
Assistência Técnica Acadêmica
Serviço de Pós-Graduação

ANOS
FOB-USP
• 1962 - 2022 •

FOLHA DE APROVAÇÃO

Dissertação apresentada e defendida por
PEDRO RODRIGUES MINIM
e aprovada pela Comissão Julgadora
em 14 de julho de 2022.

Prof. Dr. **PAULO NORONHA LISBOA FILHO**
UNESP

Prof. Dr. **CARLOS ALBERTO FORTULAN**
EESC-USP

Prof.ª Dr.ª **ANA FLÁVIA SANCHES BORGES**
FOB - USP

Prof. Dr. **JOSE HENRIQUE RUBO**
Presidente da Banca
FOB - USP

Marco A H Duarte

Prof. Dr. Marco Antonio Hungaro Duarte
Presidente da Comissão de Pós-Graduação
FOB-USP

DEDICATÓRIA

Dedico está dissertação aos meus pais, **Luis Antonio Minim** e **Valéria Paula Rodrigues Minim**, por serem sempre exemplos do tipo de professor que quero ser, e por sempre apoiarem meus sonhos. Sem eles nada disso seria possível.

Dedico também a minha irmã **Júlia**, pelo carinho, suporte e por sempre estar ao meu lado. Te amo!

AGRADECIMENTOS

Agradeço primeiramente a **Deus**, que em sua infinita sabedoria sempre colocou Bauru em minha vida, me guiou até aqui e me deu as ferramentas necessárias para ultrapassar as dificuldades desta jornada.

Ao **Prof. Dr. José Henrique Rubo**, meu orientador, por ter me recebido, pela paciência, disponibilidade e generosidade. Obrigado por todos os ensinamentos.

À **Profa. Dra. Ana Flávia Sanches Borges**, obrigado por ter me recebido em seu laboratório e ter me ajudado durante toda minha pesquisa. Graças à senhora descobri o amor por materiais dentários.

A todos que ajudaram na realização deste trabalho em especial aos Professores Doutores **Carlos Alberto Fortulan**, **Paulo Noronha Lisboa Filho**, **Rafael Salomão** e **Celso Antônio Goulart**. A ajuda de vocês foi imprescindível para a conclusão deste trabalho.

À **Faculdade de Odontologia de Bauru — USP**, em nome da **Profa. Dra. Marília Afonso Rabelo Buzalaf**, diretora da FOB. A cada dia que passo nesta universidade, sei que escolhi o caminho e o lugar certo.

Ao **Departamento de Prótese da FOB-USP**, representado pela **Profa. Dra. Ana Lúcia Pompéia Fraga de Almeida** e aos demais professores doutores: **Estevam Augusto Bonfante**, J**oel Ferreira Santiago Junior, Karin Hermana Neppelenbroek**, **Luiz Fernando Pegoraro**, **Paulo César Rodrigues Conti**, **Pedro César Garcia de Oliveira**, **Simone Soares**, **Vinícius Carvalho Porto**. Obrigado por tudo o que me ensinaram.

Agradeço às agências de fomento à pesquisa, **CNPq e FAPESP**. O presente trabalho foi realizado com o apoio do Conselho Nacional de Desenvolvimento Científico e Tecnológico (CNPq) — **Processo do Beneficiário: 133725/2020-0** e auxílio pesquisa da Fundação de Amparo à Pesquisa do Estado de São Paulo, processo **#2018/23639-0.**

Aos meus pais, **Luis** e **Valéria**, pelo suporte e carinho diário, por me incentivarem pela busca constante pelo conhecimento. Obrigado por me apoiarem mesmo quando quis mudar completamente os meus planos e por mostrarem que estão comigo todos os dias da minha vida mesmo eu estando tão longe de casa.

A minha irmã **Júlia**, por estar sempre comigo e por poder comemorar com você todas as nossas conquistas. Agradeço a Deus por ter você como minha irmã.

A **Carol**, minha namorada, pelo carinho e companheirismo. Você me inspira diariamente com sua força, dedicação e por fazer todos à sua volta melhores. Obrigado por acreditar em mim e por estar ao meu lado todos os dias. Do seu lado, tudo é mais gostoso. Bauru é muito melhor com você do meu lado. "N".

Aos meus avós, **José**, **Hélio** e **Nair** (*in memorian*), por todo o carinho, por sempre terem me incentivado e por estarem comigo todos os dias, mesmo que apenas em pensamento.

A vovó **Lela**, pelo carinho, suporte e pelo exemplo de força que a senhora é para todos ao seu redor.

Aos meus padrinhos, tia **Beth** e tio **Humberto**, pelo apoio, pelo carinho e por terem me recebido em sua casa, quando pela primeira vez saí de Viçosa.

Aos meus tios **Lena**, **Nando** e **Juninho**, por sempre acreditarem, apoiarem e torcerem por mim.

Ao meu tio **Julinho**, pela amizade, pelo apoio e por despertar em mim a vontade de ser dentista e o amor pela Reabilitação Oral.

A **Cleide**, **Paulo**, **Guilherme**, **Samira** e **Rodolfo**, por terem me recebido em Campinas quando me mudei de Piracicaba. Muito obrigado por me fazerem sentir como um filho e um irmão.

Aos amigos da T-55, em especial aos companheiros de república **Márcio**, **Vitti**, **Luiz** e **Presida**, e também ao **Sabiá**, **Meloto**, **Mateuzu**, **Férão**, **Lucão**, **Ceará** e **Cintia**. Por todos os anos de amizade, por todos os churrascos na rep, todas as tardes no bar do Alcindo e perrengues que passamos juntos na FOP. Agradeço à Deus por tornar, a cada ano, nossa amizade cada vez mais forte.

A **Júlia** e ao **Diego** (*in memorian*), pela amizade, companheirismo e por estarmos sempre juntos nos bons momentos e nas adversidades. Vocês tornaram os momentos mais difíceis, muito mais leves.

A melhor força tarefa que poderia existir, **Lucas José de Azevedo Silva**, **Brunna Mota Ferrairo**, **Raphaelle Santos Monteiro** e **Letícia Florindo Pereira**, obrigado pela amizade, pelas risadas, pelos cafés e todos os dias que tivemos juntos. Agradeço a ajuda que me deram durante o mestrado, com vocês aprendo muito todos os dias.

Aos amigos do mestrado, **Amanda**, **Camila**, **Eliezer**, **Gabriela**, **Karolyn**, **Laura**, **Maria Emilia**, **Mariana**, **Matheus**, **Sandy** e **Tatiana** por dividirem comigo as alegrias e dificuldades nesses dois anos de mestrado.

Aos funcionários da **Faculdade de Odontologia de Bauru**, em especial **Alcides**, **Cleide, Deborah**, **Elizio**, **Hebe**, por sempre estarem prontos para ajudar no que fosse necessário.

“Cuidemos do nosso coração porque é de lá que sai o que é bom e ruim, o que constrói e destrói.”

Papa Francisco

RESUMO

A hidroxiapatita (HA) proveniente de estrutura óssea bovina tem elevada importância dentre os biomateriais devido à sua biocompatibilidade e bioatividade. Entretanto, as cerâmicas densas de hidroxiapatita bovina apresentam propriedades mecânicas insuficientes para a confecção de infra-estuturas de prótese fixa. O presente estudo objetivou avaliar o efeito da adição de polivinilbutiral (PVB) e ácido esteárico (AE) e de duas metodologias de sinterização (*2-step* e convencional), nas propriedades mecânicas de biocerâmica densa policristalina de HA de origem bovina. Dessa forma, a partir de um esquema fatorial 2x2, 4 grupos foram avaliados. Para tanto, a HA foi extraída de ossos bovinos, calcinados a 900 °C, nanoparticuladas em moinho de bolas e submetida à prensagem uniaxial estática em discos, conforme a norma ISO 6872. Os grupos submetidos a sinterização convencional (HAAC e HASC) tiveram pico máximo de temperatura de 1300 °C e resfriamento lento até a temperatura ambiente. Já os grupos com sinterização *2-step* (HAA2 e HAS2), tiveram pico máximo de 950 °C com resfriamento rápido para 880 °C e posterior resfriamento lento a temperatura ambiente. As amostras dos 4 grupos foram caracterizadas por difratometria de raios-x (DRX), análise térmica diferencial (DTA) e espectroscopia de infravermelho por transformada de Fourrier (FTIR), e avaliadas pelos testes de microscopia eletrônica de varredura (MEV) densidade relativa, através do princípio de Arquimedes, pelo teste de resistência à flexão biaxial e pela análise do módulo de elasticidade. Os valores obtidos de densidade relativa e resistência à flexão foram submetidos ao teste de normalidade de Shapiro-Wilk e a partir disso foi realizado teste de Kruskal-Wallis e pós teste de Dunn, para todos os testes. Foi possível concluir que as cerâmicas de HA submetidas a sinterização convencional e sem a adição de aglutinantes obteve melhores propriedades mecânicas que os demais grupos.

Palavras-chave: durapatita; cerâmica; materiais biocompatíveis

ABSTRACT

Effects of the sintering parameters and the addition of agglutinants on the structural characteristics of bovine hydroxyapatite dense bioceramics

Hydroxyapatite (HA) from bovine bone structure has high importance among biomaterials due to its biocompatibility and bioactivity. However, hydroxyapatite dense ceramics have inadequate mechanical properties for their intended purpose. The present study aimed to evaluate the effect of the addition of polyvinyl butyral (PVB) and stearic acid (SA) and two sintering methodologies (*2-step* and conventional) on the mechanical properties of bovine hydroxyapatite dense polycrystalline bioceramic. Thus, from a 2x2 factorial scheme, 4 groups were evaluated. Therefore, HA was extracted from bovine bones, turned into nanoparticles in a ball mill and subjected to uniaxial and isostatic pressing into discs, according to the ISO 6872 standard. The groups submitted to conventional sintering (HAAC and HASC) had a maximum temperature peak of 1300 °C and slow cooling to room temperature. The groups with *2-step* sintering (HAA2 and HAS2) had a maximum peak of 950 °C with rapid cooling to 880 °C and subsequent slow cooling to room temperature. The samples of the 4 groups were characterized by x-ray diffractometry (XRD), differential thermal analysis (DTA) and Fourrier transform infrared spectroscopy (FTIR), and evaluated by scanning electron microscopy (SEM) relative density, through the Archimedes principle, by the biaxial flexural strength test and by the analysis of the modulus of elasticity. The values obtained for relative density and flexural strength were submitted to the Shapiro-Wilk normality test and from there, the Kruskal-Wallis test and Dunn's post-test were performed for all tests. It was possible to conclude that the HA ceramics submitted to conventional sintering and without the addition of binders obtained better mechanical properties than the other groups.

Keywords: durapatite; ceramics; biocompatible materials

LISTA DE FIGURAS

LISTA DE TABELAS

Sumário

Introdução

1. INTRODUÇÃO

A indústria frigorífica desempenha um papel socioeconômico importante no Brasil. Em 2020, o país alcançou mais uma vez o posto de maior exportador de carne do mundo, com 2,2 milhões de toneladas, fornecendo cerca de 14,4% do total de exportações mundiais, além de possuir o segundo maior rebanho do mundo, detendo 232 milhões de cabeças de gado, havendo ainda uma tendência de crescimento para os próximos anos (1) Em contrapartida, sua magnitude gera preocupações ambientais e de saúde pública, devido à abundante quantidade de resíduos gerados (2–5).

Para alcançar uma produção sustentável e de menor impacto ambiental é necessário o reaproveitamento desses resíduos. Os ossos, representantes da maior porção destes rejeitos, são formados por uma fase inorgânica (mineral) e uma fase orgânica. A fase biomineral, composta principalmente por hidroxiapatita carbonatada, compreende 65 – 70% do osso, a água responde por 5 – 8% e a fase orgânica, que está principalmente na forma de colágeno, é responsável pela porção restante (6–10). Esse resíduo, devido ao seu alto valor nutricional, rico em cálcio e proteínas, tem sido reaproveitado na produção de farinhas nutritivas voltadas à alimentação animal ou como adubo orgânico (11,12). Entretanto, esta forma de reaproveitamento gera produtos com baixo valor agregado, dado que o principal componente mineral dos ossos é a hidroxiapatita (HA) e este material é de grande interesse em diversas áreas.

A hidroxiapatita pode ser utilizada, por exemplo, para fins médicos como no reparo de áreas com perdas ósseas (11,13–15) e no revestimento de implantes que apresentem alta taxa de degradação (16). Já na farmacêutica, este material pode ser utilizado na forma de agente de liberação de drogas (17–19) em locais específicos e para liberação lenta e sustentada de fármacos. Na indústria química, a HA pode ser utilizada como fase estacionária em colunas cromatográficas utilizadas para separação de proteínas e ácidos nucleicos (20) Segundo Ibrahim et al. (11) (2020), com o desenvolvimento de novas e melhores formas de eliminação da poluição do ar, do solo e da água, o uso de HA pode ser altamente benéfico para remoção de contaminantes presentes nas fases gasosa, líquida e sólida.

Já na Odontologia, dentre as diversas aplicações da hidroxiapatita, destacam-se os enxertos ósseos particulados, que visam evitar e recuperar perdas ósseas relacionadas à extração de dentes, casos graves de doença periodontal e em correções bucomaxilofaciais, além da cobertura de implantes dentários e no desenvolvimento de novas cerâmicas odontológicas (21–24).

A utilização da hidroxiapatita bovina, além de aumentar o valor agregado dos rejeitos da indústria de corte, vem ao encontro do crescente interesse em reduzir o custo associado a HA sintética, visto que a produção de HA por fontes naturais corresponde a uma fração do custo de produção pela via sintética (10,25–28)Além disso, os cristais de hidroxiapatita bovina são de tamanho nanométrico, com comprimento médio de 50 nm, largura de 25 nm e espessura de 2 a 5 nm. Essas pequenas dimensões e a baixa cristalinidade são duas características que diferem as HA bovinas das obtidas de outras fontes, como as sintéticas e as minerais (29,30).

A HA possui como fórmula química: $Ca_{10}(PO_4)(OH)_2$; apresenta uma razão de Ca/P de 1,67 e suas principais características são: osteocondução, biocompatibilidade e bioatividade. A osteocondutividade ocorre devido à capacidade da hidroxiapatita formar ligações químicas com os ossos, que, por sua vez, aumenta a velocidade de formação de uma nova estrutura óssea ao redor de implantes, consequentemente aumentando a velocidade de cicatrização. A bioatividade ocorre devido a devido à sua similaridade química em relação à fração mineral do osso humano. Além disso, a HA é biocompatível, ou seja, não tóxica, não inflamatória e em pH fisiológico, está em equilíbrio com o meio (31–35).

As cerâmicas densas de hidroxiapatita, no entanto, apresentam pobres propriedades mecânicas. Seus valores resistência à tração, resistência à compressão e resistência à flexão de cerâmicas HA densas estão na faixa de 38–300 MPa, 120–900 MPa e 38–250 MPa, respectivamente, sendo cerca de três vezes menores que os valores associados ao osso humano (36).

As propriedades mecânicas variam com a metodologia de manufatura das cerâmicas. Dentre as etapas da manufatura de cerâmicas de HA, estão a moagem, a adição de ligantes, a secagem dos pós precursores, a prensagem e a sinterização (37).

O polivinil butiral ($(C_8H_{14}O_2)_n$) (PVB) é um ligante para meio alcoólico utilizado para cerâmicas de HA (33). Diversos estudos mostraram que a adição de

aglutinantes, como o PVB, facilita o processo de manipulação e manufatura dos espécimes verde. No entanto, sua utilização pode levar a um aumento de porosidade da cerâmica, perda de translucidez e diminuição da resistência à fratura após o processo de sinterização (38,39).

A sinterização é uma das importantes etapas do processo de manufatura, devido à sua influência em fatores como o tamanho do grão, a densificação e o tamanho dos poros presentes na cerâmica (36,40–42).

Várias técnicas de sinterização de HA foram desenvolvidas nos últimos anos, dentre elas: sinterização em fornos muflas convencionais, sinterização por micro-ondas e o método de plasma de faísca (42). Independente da metodologia de sinterização aplicada, o gradiente de temperatura utilizado é capaz de alterar significativamente as propriedades mecânicas do material.

Temperaturas de sinterização mais baixas têm sido adotadas visando garantir melhor bioatividade de cerâmicas de HA e regimes de temperatura de sinterização e tempos de permanência mais altos podem ser úteis na melhoria das propriedades mecânicas, como resistência à fratura e módulo de elasticidade, mas podem causar aumento do tamanho dos grãos (43).

Segundo Canillas et al. (40) (2017) o aumento do grão durante o processo de sinterização pode ser prejudicial para as características mecânicas da cerâmica final. Desta forma, os efeitos da temperatura de sinterização nas propriedades mecânicas da HA ainda não estão totalmente elucidados havendo a necessidade de pesquisas para o completo entendimento (42).

Diversos autores defendem a adoção da sinterização via *2-step*, visando melhorar as propriedades mecânicas da HA a partir da utilização tanto de uma temperatura de sinterização mais baixa quanto de um maior tempo de permanência. Essa metodologia apresentou grande interesse também devido ao seu baixo custo de implementação, visto que, por não ser necessário o uso de fornos com alta pressão ou campo elétrico, o procedimento se torna factível em fornos utilizados para sinterização convencional (44–49).

O *2-step* se baseia em elevar a temperatura de uma amostra até uma temperatura inicial, de modo que o sistema alcance energia suficiente para que a amostra atinja uma densidade intermediária (cerca de 75% da densidade teórica), seguida de um rápido resfriamento e manutenção a uma temperatura mais baixa até que a densificação seja concluída (46).

Considerando a literatura existente percebe-se que o conhecimento dos efeitos da adição de aglutinantes e dos métodos de sinterização (convencional e *2-step*) nas propriedades mecânicas da HA ainda não estão completamente elucidados, havendo a necessidade de pesquisas para o seu completo entendimento. Sendo assim, o presente estudo visou avaliar o efeito da adição de aglutinantes e de diferentes metodologias de sinterização nas propriedades mecânicas de biocerâmica densa policristalina de hidroxiapatita bovina.

Artigo

2. ARTIGO

The article presented in this dissertation was written according to the **Dental Materials** instructions and guidelines for article submission

Effects of the sintering parameters and the addition of agglutinants on the structural characteristics of bovine hydroxyapatite dense bioceramics

Authors:

Pedro Rodrigues Minim

Department of Prosthodontics and Periodontics, Bauru School of Dentistry, University of São Paulo, Bauru, SP, Brazil.

Lucas José de Azevedo Silva

Department of Prosthodontics and Periodontics, Bauru School of Dentistry, University of São Paulo, Bauru, SP, Brazil.

Brunna Mota Ferrairo

Department of Operative Dentistry, Endodontics and Dental Materials, Bauru School of Dentistry, University of São Paulo, Bauru, SP, Brazil.

Leticia Florindo Pereira

Department of Prosthodontics and Periodontics, Bauru School of Dentistry, University of São Paulo, Bauru, SP, Brazil.

Celso Antônio Goulart

Department of Physics, School of Sciences, São Paulo State University, Bauru, Brazil.

Raphaelle Santos Monteiro

Department of Prosthodontics and Periodontics, Bauru School of Dentistry, University of São Paulo, Bauru, SP, Brazil.

Paulo Noronha Lisboa Filho

Department of Physics, School of Sciences, São Paulo State University, Bauru, Brazil

Carlos Alberto Fortulan

Department of Mechanical Engineering, São Carlos School of Engineering, University of São Paulo, São Carlos - SP, Brazil.

Ana Flávia Sanches Borges

Department of Operative Dentistry, Endodontics and Dental Materials, Bauru School of Dentistry, University of São Paulo, Bauru, SP, Brazil.

José Henrique Rubo

Department of Prosthodontics and Periodontics, Bauru School of Dentistry, University of São Paulo, Bauru, SP, Brazil.

ABSTRACT

Hydroxyapatite (HA) from bovine bone structure has high importance among biomaterials due to its biocompatibility and bioactivity. However, hydroxyapatite dense ceramics have inadequate mechanical properties for their intended purpose. The present study aimed to evaluate the effect of the addition of polyvinyl butyral (PVB) and stearic acid (SA) and two sintering methodologies (*2-step* and conventional) on the mechanical properties of bovine hydroxyapatite dense polycrystalline bioceramic. Thus, from a 2x2 factorial scheme, 4 groups were evaluated. Therefore, HA was extracted from bovine bones, cancined and turned into nanoparticles in a ball mill and subjected to uniaxial and isostatic pressing into discs, according to the ISO 6872 standard. The groups submitted to conventional sintering (HAAC and HASC) had a maximum temperature peak of 1300 °C and slow cooling to room temperature. The groups with *2-step* sintering (HAA2 and HAS2) had a maximum peak of 950 °C with rapid cooling to 880 °C and subsequent slow cooling to room temperature. The samples of the 4 groups were characterized by x-ray diffractometry (XRD), differential thermal analysis (DTA) and Fourrier transform infrared spectroscopy (FTIR) and evaluated by scanning electron microscopy (SEM) relative density, through the Archimedes principle, by the biaxial flexural strength test and by the analysis of the modulus of elasticity. The values of the data obtained for relative density and flexural strength were submitted to the Shapiro-Wilk normality test and from there, the Kruskal-Wallis test and Dunn's post-test were performed for all tests. It was possible to conclude that the HA ceramics submitted to conventional sintering and without the addition of binders obtained better mechanical properties than the other groups.

Keywords: durapatite; ceramics; biocompatible materials

2.1. INTRODUCTION

The socio-economic importance of the meatpacking industry is undeniable, however its ability to generate pollutants has caused environmental concerns worldwide. Solutions are needed so that waste from this sector has a correct and sustainable destination (1–5).

Bovine bones represent the largest portion of these wastes and their reuse can significantly contribute to reducing the environmental impact (2,3,50). The main mineral component of bones is hydroxyapatite (HA), one of the most promising biomaterials and of great interest in several areas (11,13–20).

Among the various applications of hydroxyapatite in Dentistry, particulate bone grafts stand out, which aim to prevent and recover bone losses related to tooth extraction, severe cases of periodontal disease, and in oral and maxillofacial corrections, in addition to covering dental implants and in the development of new dental ceramics (21–23,33).

HA has a chemical formula $Ca_{10}(PO_4)(OH)_2$ and its main characteristics are: osteoconduction, biocompatibility and bioactivity. However, HA has poor mechanical properties, restricting its applications to situations where high loading forces are not required (51–56).

The tensile strength, compressive strength, and flexural strength values of dense HA ceramics are in the range of 38–300 MPa, 120–900 MPa, and 38–250 MPa, respectively, being about three times lower than the values associated with the human bone (36). These properties vary with the ceramic manufacturing methodology (milling, presence of binders, drying of the precursor powders, pressing and sintering) (44–49).

Several studies have shown that the addition of binders such as polyvinyl butyral (PVB), a binder for alcoholic media used for HA ceramics (33), facilitates the process of handling and manufacturing the specimens in green. However, its use can lead to an increase in ceramic porosity, loss of translucency and a decrease in fracture resistance after the sintering process (38,39).

The sintering temperature influences the grain size, the densification and the size of the pores present in the ceramic (36,40–42). Lower sintering temperatures

have been adopted to ensure better bioactivity of HA ceramics. Higher sintering temperature regimes and residence times can be useful in improving mechanical properties, such as fracture strength and elastic modulus, but can also cause grain size to increase (43). According to Canillas et al. (40) (2017), the increase in the size of the grain during the sintering process can be detrimental to the mechanical characteristics of the final ceramic.

Aiming to guarantee smaller grains in the search to improve the mechanical properties, several authors defend the adoption of sintering via *2-step*, a methodology that is based on raising the temperature of a sample to an initial temperature, so that the system reaches sufficient energy for the sample reaches an intermediate density (about 75% of theoretical density), followed by rapid cooling and holding at a lower temperature until densification is complete (45).

Considering the existing literature, it is clear that the knowledge of the effects of the addition of binding agents and the sintering temperature on the mechanical properties of HA is not yet fully elucidated, and there is a need for research to fully understand it. Therefore, the present study aimed to evaluate the effect of the addition of binders and of different sintering methodologies on the mechanical properties of dense polycrystalline bovine hydroxyapatite (HA) bioceramics.

2.2. MATERIAL AND METHODS

2.2.1. Experimental design

The present *in vitro* study used a 2×2 factorial design scheme (sintering, binder). The sintering levels evaluated were the conventional and *2-step* strategies and those of binder were presence and absence, totalling 4 groups of HA bioceramics (Table 1). The groups were designed with the objective of evaluating physically, mechanically and structurally, sintered HA bioceramics.

Table 1- Study groups and their respective descriptions

Study groups	Description
HAAC	Hydroxyapatite ceramic with binder and conventional sintering
HAA2	Hydroxyapatite ceramic with binder and *2-step* sintering
HASC	Binder-free hydroxyapatite ceramic with conventional sintering
HAS2	Binder-free hydroxyapatite ceramic with *2-step* sintering

Source: Elaborated by the author

2.2.2. HA Ceramic Manufacture

(Adapted from 26)

The manufacture of HA dense bioceramics was carried out in the Biomaterials II laboratory of the Integrated Research Centre of the Bauru School of Dentistry of the University of São Paulo, and in the Composites and Tribology Laboratory of the São Carlos School of Engineering of the University of São Paulo.

HA was obtained from bovine metatarsals, from Nellore animals, screened by the Brazilian System of Bovine and Bubaline Traceability (SISBOV). The bone tissue was fractionated and subjected to thermochemical processes, where the bone pieces were submerged in hydrogen peroxide (H_2O_2) at 100 volumes under heating with a Bunsen burner, to remove organic matter. The bones were then washed with deionized water to remove H_2O_2 and taken to an oven at 800 °C for calcination and subsequent removal of the remaining organic matter.

Then the samples were sent to a laboratory accredited by the Ministry of Health where chemical and cytotoxic analyses were performed, in which it was

possible to verify the absence of heavy metals and biological contaminants, respectively.

X-ray diffractometry (XRD) and Fourier transform infrared spectroscopy (FTIR) analyses were performed to characterize the HA. The results were compared to the standard powder values (Sigma-Aldrich). Wavelength scattering x-ray fluorescence analysis (WDXRF) was also performed, which verified that the chemical composition was in accordance with ASTM F1185 (58) (2014), which determines the maximum concentration of heavy metals allowed for HA obtained from animal origin.

The materials used in the manufacture of the HA ceramics were: hydroxyapatite, polyvinyl butyral (PVB) (Butvar B98) and stearic acid (SA) as binding agents; para-aminobenzoic acid (PABA) as a deflocculant of the alcoholic system; isopropyl alcohol as a solvent for the binder and as a liquid medium for the slurry.

The milling process, which aimed to obtain a submicrometric powder, was carried out in a polyethylene jar with a height of 85 mm and a volume of 300 cm^3 loaded with 45 vol.% apparent (500 g) of grinding elements (3- YTZP with a diameter of 10 mm). In the groups with the addition of binder, PVB and SA were added, aiming to confer plasticity and resistance to green after conformation. The jar was loaded with a slurry at a concentration of 30 vol.% of solids, making a useful volume of 100 mL and placed in a ball mill at a speed of 104 rpm for 48 hours and in a vibrating mill for 72 hours.

Two types of grinding were performed in an alcoholic medium. In the first milling, a jar was charged with 30 vol.% of Hydroxyapatite, 70 vol.% of isopropyl alcohol and 0.05 wt% of PABA (para-aminobenzoic acid) and placed for 48 hours in a ball mill and 72 hours in a vibrating mill. After this period, 1.2 wt% of PVB, previously dissolved in isopropanol in a proportion of 1:10 on the weight of HA and 0.05% of SA, were added to the groups with the addition of binders, mixed and homogenized in a vibrating mill. of balls for two hours.

For all groups, with or without binders, the jar was unloaded and the slurry was dried in a kiln at 80 °C. All prepared powders were granulated and graded on #200 mesh stainless steel meshes (≤ 75 μm). Then, the powders were weighed and separated into 0.5 g each for the preparation of disc-shaped specimens, and 1.5 g for bar-shaped specimens. Each disk was 15 mm in diameter x 1.4 mm in height and each bar was 21 mm in length x 4 mm in width x 3 mm in height, after being

subjected to uniaxial pressing at 100 MPa for 1 minute and an isostatic pressing at 200 MPa for 1 more minute, as recommended by ISO 6872 (59) (2015).

The sintering of the specimens was performed in a Lindberg Blue/M chamber oven at atmospheric pressure.

The groups, HAAC and HASC, subjected to the conventional sintering scheme followed the following heating ramp (Figure 1):

1. From room temperature to 160 °C with heating rate of 2.7 °C/min;
2. From 160 °C to 600 °C at 4°C/min;
3. From 600 °C to 1100 °C at 5°C/min;
4. From 1100 °C to 1300 °C at 6°C/min
5. The final temperature will be maintained for 120 minutes;
6. Slow cooling to room temperature.

Figure 1- Conventional sintering heating ramp

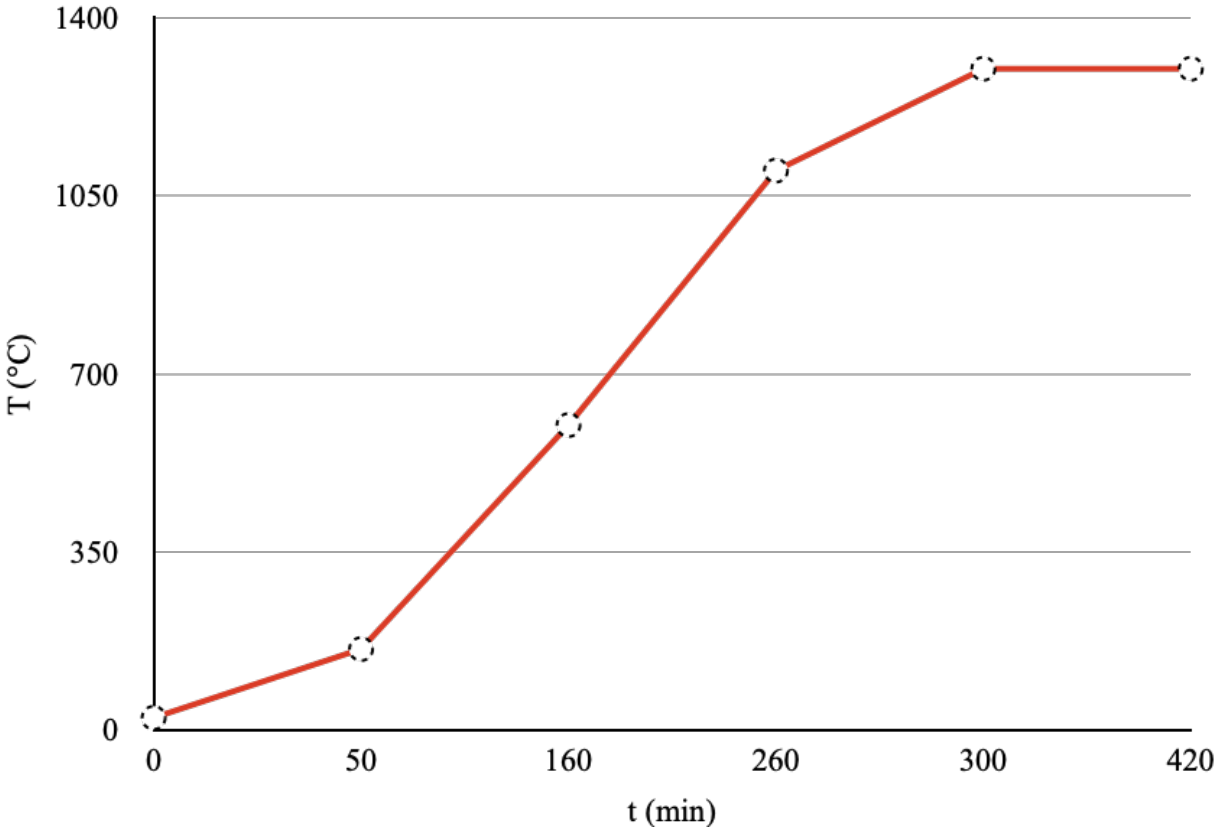

Source: Elaborated by the author

On the other hand, the groups, HAA2 and HAS2, subjected to the *2-step* sintering scheme followed the following heating ramp, based on the model proposed by Lourenço et al. (45) (2011) (Figure 2):

1. From room temperature to 600 °C with heating rate of 2 °C/min;
2. The temperature remained stable for 30 minutes;
3. From 600 °C to 950 °C with a heating rate of 5 °C/min;
4. From 950 °C to 880 °C with a cooling rate of 20 °C/min;
5. The temperature of 880 °C was maintained for 12 hours;
6. Slow cooling to room temperature.

Figure 2- *2-step* sintering heating ramp

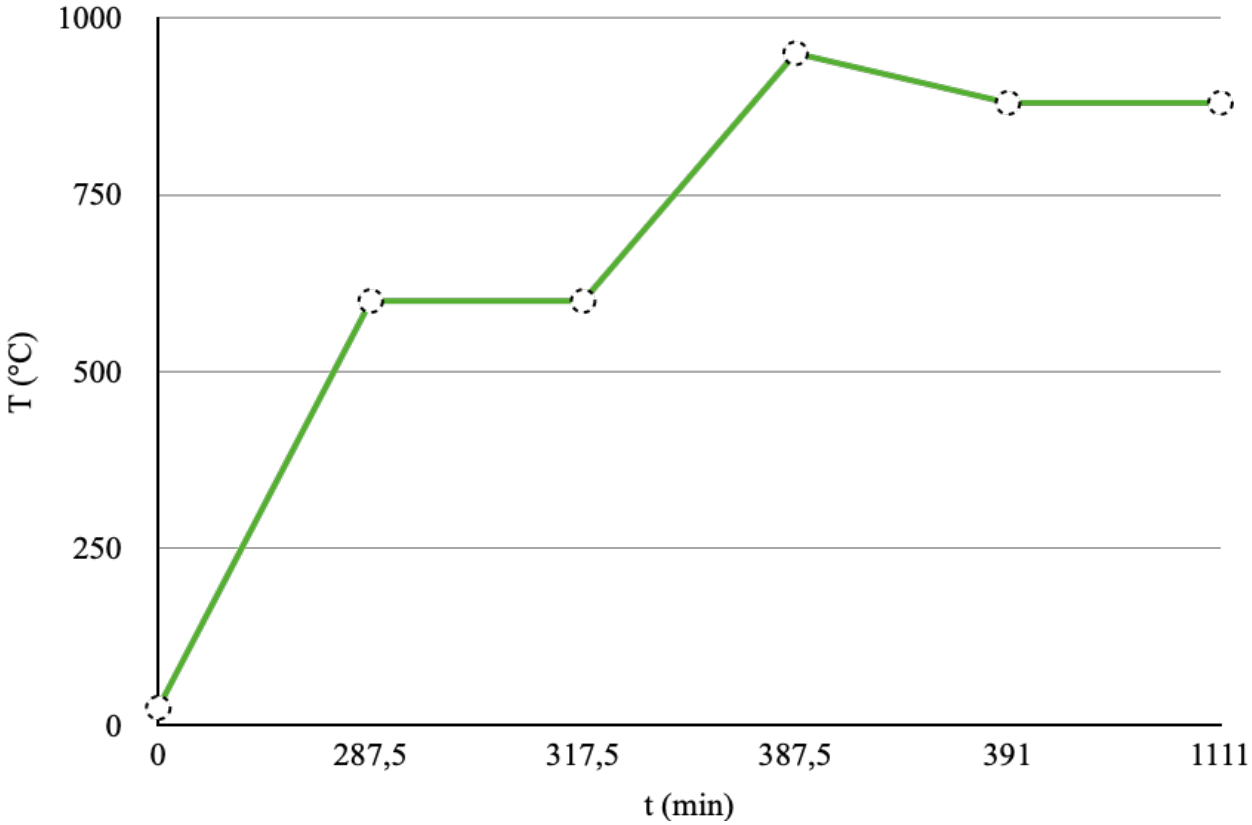

Source: Elaborated by the author

2.2.3. Laboratory Tests

2.2.3.1. *Thermal Analysis: Thermogravimetry (TG), Differential Thermal Analysis (DTA)*

(Adapted from (60))

Considering the importance of determining the thermal behaviour and contraction of the starting powders for the manufacture of ceramics, the Thermal Analysis (TG/DTA) (STA 409, Netzsch) was performed. The Hydroxyapatite starting powders, with or without binding agent simultaneous results of TG-DTA were obtained for each material under study.

About 5 mg of each sample was weighed and placed in an alumina crucible. The parameters were set at a constant heating rate in a dry air atmosphere.

2.2.3.2. *X-Ray Diffraction (XRD)*

X-ray diffraction to identify the crystalline phases present was performed on the sintered samples of each group. Using the Shimadzu X-ray diffractometer model XDR 7000, in the Bragg-Brentano setup using Cu kαlλ=1.54060 Å, coλ=1.54060 Å, a goniometer θ-θ, angular scan between 10° e 70°, with a sweep speed of 2° / min, the source of copper kα radiation being accelerated with a potential of 40 kV and a current of 30 mA.

The crystalline phases were identified by comparing the spectra obtained with the standard sheets from the JCPDS database (Joint Committee on Powder Diffraction Standards) using the Crystalographica Search-Match program.

2.2.3.3. *Fourier Transform Infrared Spectroscopy (FTIR)*

In order to perform Fourier Transform Infrared Spectroscopy, disk-shaped samples were placed in an FTIR spectrometer (IRPrestige 21, Shimadzu Corporation, Kyoto, Honshu, Japan) attached to an Attenuator of Total Reflection (ATR) device (Smart Miracle™) containing a diamond plate, (Pike Technologies, Madison, Wisconsin, USA). Prior to each reading, each compound was pressed

against the ART diamond crystal using a low micrometre pressure clamp (408 psi) to allow optimal contact of the compounds with the diamond crystal. The transmittance spectrum was obtained between 4000 and 450 cm^{-1} with 32 scans at 4 cm^{-1}.

2.2.3.4. *Scanning Electron Microscopy (SEM) and Energy Dispersion X-ray Spectroscopy (EDS)*

Morphological and chemical analyses were performed by scanning electron microscopy (SEM) and energy scattering x-ray spectroscopy (EDS), respectively.

The analyses were carried out in a Scanning Electron Microscope (JEOL-JSM 5600LV, Tokyo, Japan) and morphologically evaluated to visualize, under 1000x, 2000x and 5000x magnification, the shape and size of the particulate HA powder grains, in addition to all experimental groups after sintering.

To perform the EDS, the scanning electron microscope was equipped with an X-ray detector (Voyager, Noran Instruments), operated under vacuum and in back-scattered electron mode. The instrument contains an ultra-thin Norvar window that functions as a Windows NT-based digital microanalysis system.

2.2.3.5. *Density*

The determination of the density of the sintered ceramic bodies was carried out using the method based on the Archimedes principle, according to Associação Brasileira de Normas Técnicas (ABNT) NBR 16661 (61) (2017). The method consists of boiling the samples in ultrapure water for one hour to remove air and impurities from the pores, such as unconsolidated powders. The samples were cooled to room temperature and weighed, obtaining measurements of wet mass (mw), immersed mass (mi) (in ultrapure water) and dry mass (md). To measure the dry mass, the samples were kept in an oven at about 100°C for a period of two hours. Based on m_w, m_i, m_d and ρ_e (liquid specific mass), calculations were performed using equations eq.(1) for apparent volume, eq.(2), for porosity, eq.(3), for density.

$$V_a = \frac{(m_w - m_i)}{\rho_e} \quad (1)$$

$$P_a(\%) = \frac{m_w - m_d}{m_w - m_i} * 100 \quad (2)$$

$$D_a = \frac{m_d}{AP} \quad (3)$$

Relative density was calculated using eq. (4). The actual density of hydroxyapatite powder ($D_{100\%}$) was determined by pycnometry. For this purpose, a container made of material with a low coefficient of expansion (pycnometer) was weighed and subsequently filled with a liquid solution of hydroxyapatite using distilled water at 24 °C. The calculation was performed using the mass obtained according to the already known volume.

$$D_r = \frac{D}{D_{100\%}} * 100 \quad (4)$$

Where:

D_r is relative density in percentage,

D is the density of the material obtained after the density test,

$D_{100\%}$ corresponds to 3.28 gcm3, a value obtained from the pycnometric test.

2.2.3.6. *Biaxial flexural fracture resistance*

The biaxial flexural strength test was performed with the disc-shaped specimens. The device used for the test has support for the specimen with three spheres (1 mm in diameter), distributed in a circumference of 10 mm in diameter and equidistant at an angle of 120º, according to the standards of ISO 6872 (59) (2015). With the device, the test rod must be perfectly aligned with the centre of the sample. The discs were cleaned with distilled water and isopropyl alcohol. A polyethylene sheet was interposed between the base spheres and the specimen and between the piston and the specimen for uniform distribution of contact pressure. The load was applied centrally to the specimen by means of a flat-tipped piston with a diameter of

1.2 mm, at a speed of 0.5 mm/min. To calculate the biaxial flexural strength, in MPa, the eq. (5-7) was used:

$$\sigma = \frac{-0{,}2387 * P * (X - Y)}{b^2} \quad (5)$$

Where:

σ is the maximum strength (MPa),

P is the total fracture load (N),

b is sample thickness (mm),

X and Y are values calculated from the equations:

$$X = (1 + v) * In * \left(\frac{r_2}{r_3}\right)^2 + \frac{1 - v}{2} * \left(\frac{r_2}{r_3}\right)^2 \quad (6)$$

$$Y = (1 + v) * \left[1 + In * \left(\frac{r_1}{r_3}\right)^2\right] + (1 - v) * \left(\frac{r_1}{r_3}\right)^2 \quad (7)$$

Where:

v is Poisson's ratio value (if the value is not known, 0.25 will be used),

r_1 is the radius of the support circle (mm),

r_2 is the radius of the load application area,

r_3 is the radius of the specimen.

2.2.3.7. *Modulus of elasticity*

The determination of the modulus of elasticity (Young's modulus) and Poisson's ratio of the experimental materials was performed using the excitation impulse technique, according to ASTM E1876 (62) (2015), aiming at a non-destructive characterization of the samples.

For this, the Sonelastic® equipment (ATCP) and its software (ATCP Sonelastic 2.8) were used. The weight and dimensions of the specimen to be analysed were entered into the software and the specimen was placed at the base of the equipment. The material was excited using a metal rod and the sound emitted by the specimen was captured by the microphone present in the measuring device. The frequency of the emitted sound waves was then analysed by the computer and the Young's modulus and relative density data calculated.

2.2.4. Statistical analysis

The obtained results were organized in tables so they could be analysed statistically. As there was no parametric distribution, Kruskal-Wallis and Dunn's tests were used. For all cases, a significance level of 5% was adopted.

2.3. RESULTS

2.3.1. Thermal Analysis: Thermogravimetry (TG), Differential Thermal Analysis (DTA)

Differential thermal analysis, as shown in Figure 3, allowed observing the phenomena that occurred during heating of the groups with (HAA) and without binding agents (HAS). It was possible to observe a gain in mass in both groups up to about 650 °C with subsequent loss of part of the acquired mass until reaching a temperature of 1000 °C. It was also observed that during the entire heating ramp, the mass gain was more expressive in the group without binder (HAS).

Figure 3- Differential thermal analysis graph

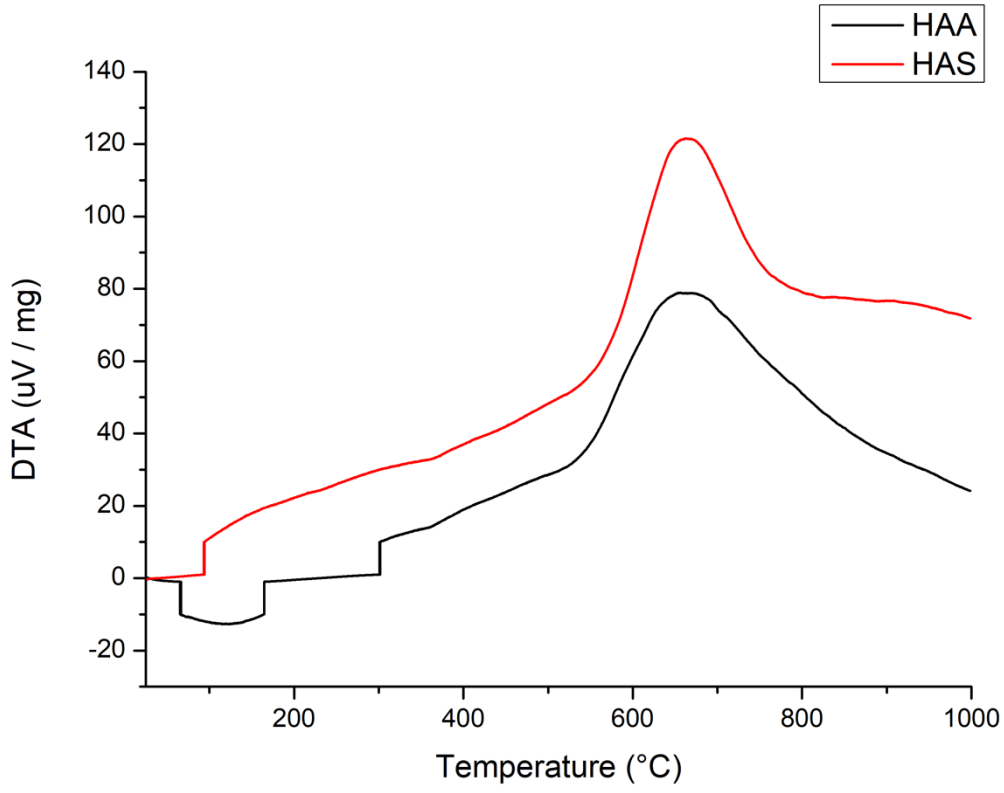

Source: Elaborated by the author

2.3.2. X-Ray Diffraction (XRD)

Figure 4 presents the results of X-ray Diffraction of the samples of the four groups evaluated. The spectra of all groups show the characteristic crystallographic peaks of HA, as shown in card no. 01-074-0565.

Figure 4- X-ray diffractometry graph

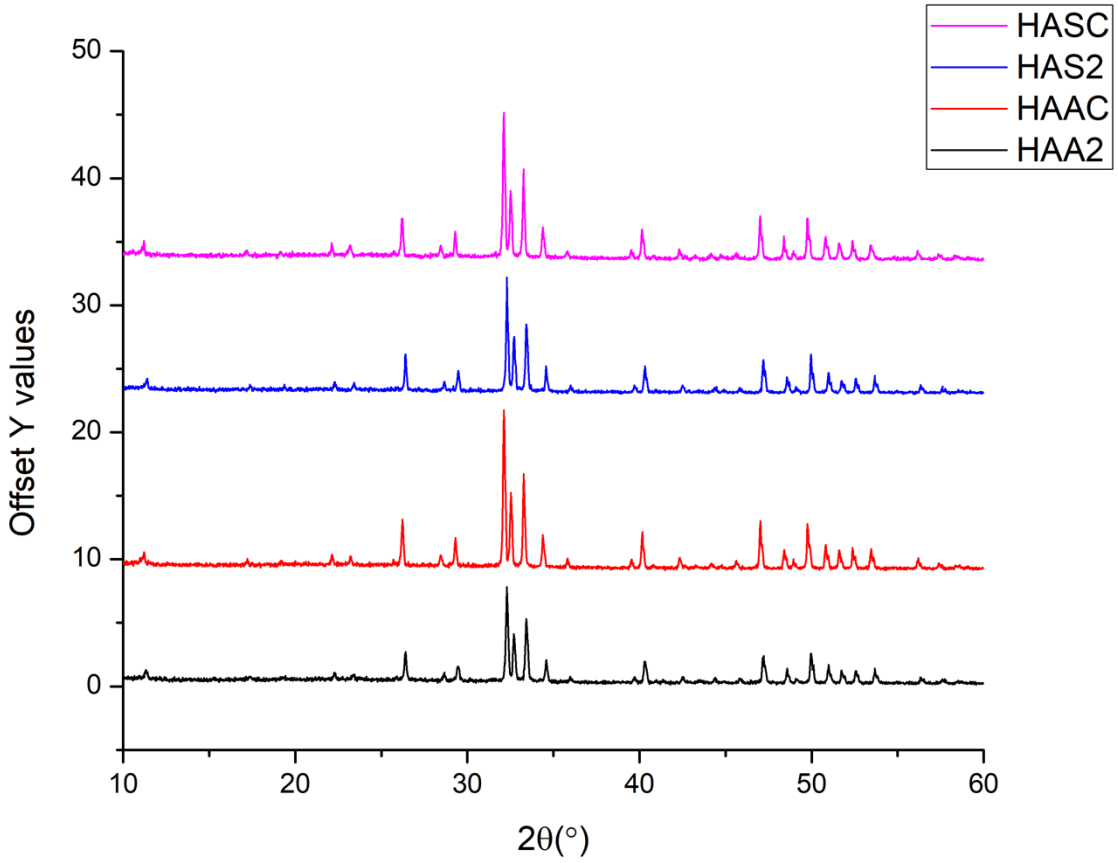

Source: Elaborated by the author

2.3.3. Fourier Transform Infrared Spectroscopy (FTIR)

The FTIR results showed, in Figure 5, all the bonds present in the materials. All samples showed bands attributed to groups $(PO_4)^{-3}$ (1101, 1026, 633 e 560 cm^{-1}), to H_2O bonds (1650 cm^{-1}), to CO_2 bonds at the time of synthesis, to the band (1545 cm^{-1}) and to the $Ca^{2+} - CO$ bond (2010 cm^{-1}) (63,64).

Figure 5- Fourier Transform Infrared Spectroscopy Graph

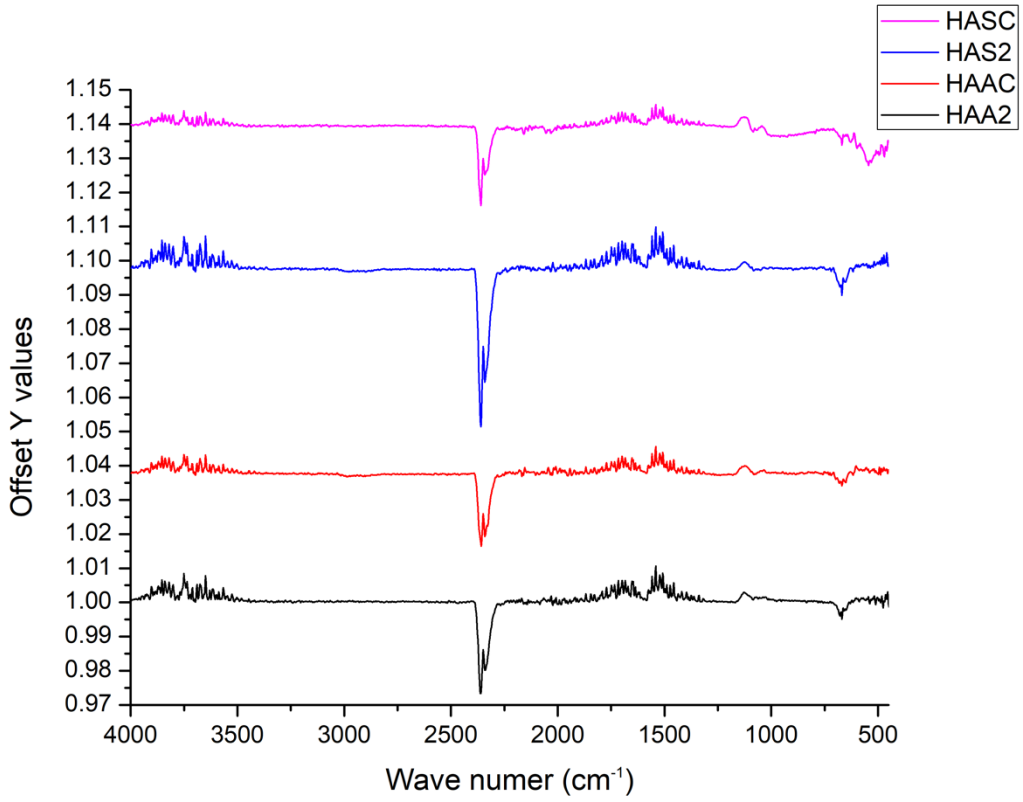

Source: Elaborated by the author

2.3.4. Scanning Electron Microscopy (SEM) and Energy Dispersion X-ray Spectroscopy (EDS)

The microstructures of the samples of the four groups evaluated are shown in Figures 6 - 13. It was possible to observe a greater cohesion of the HA grains in the groups sintered by the conventional methodology (HAAC and HASC), and consequently a greater number of pores in the groups that used the methodology 2-*step* (HAA2 and HAS2).

Comparing the groups subjected to conventional sintering (HAAC and HASC), it was possible to observe that the HASC group presented lower porosity and mostly only intra-grain pores, while HAAC presented, in addition to intra-grain pores, pores between one grain and another of HA (inter grain).

Figure 6- Surface images (x1000, x2000 and x5000) of hydroxyapatite specimen added with binders and sintered by the *2-step* method

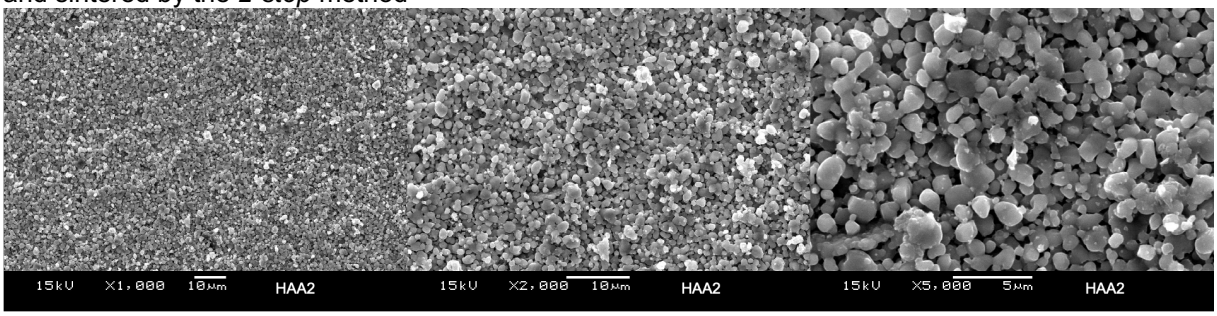

Source: Elaborated by the author

Figure 7- Surface images (x1000, x2000 and x5000) of hydroxyapatite specimen without addition of binders and sintered by the *2-step* method

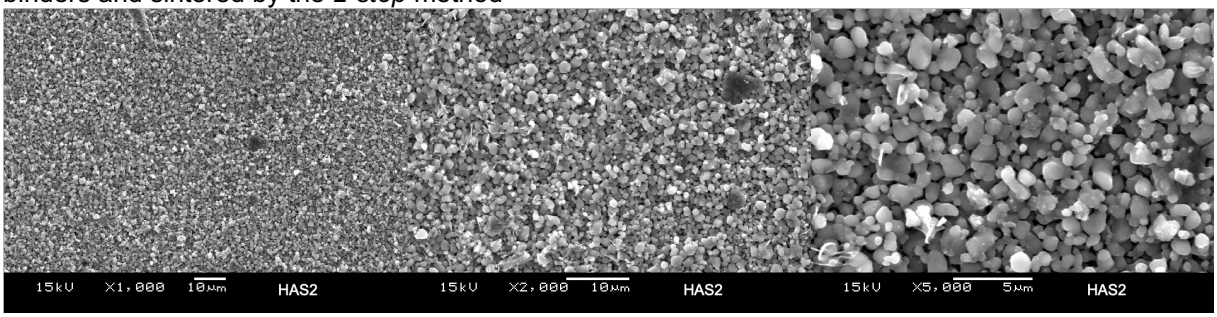

Source: Elaborated by the author

Figure 8- Surface images (x1000, x2000 and x5000) of a hydroxyapatite specimen added with binders and sintered by the conventional method

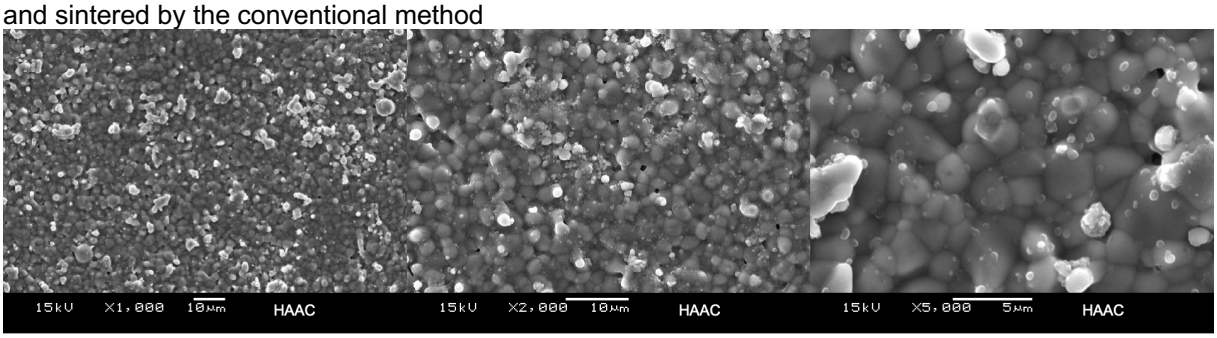

Source: Elaborated by the author

Figure 9- Surface images (x1000, x2000 and x5000) of hydroxyapatite model surface without addition

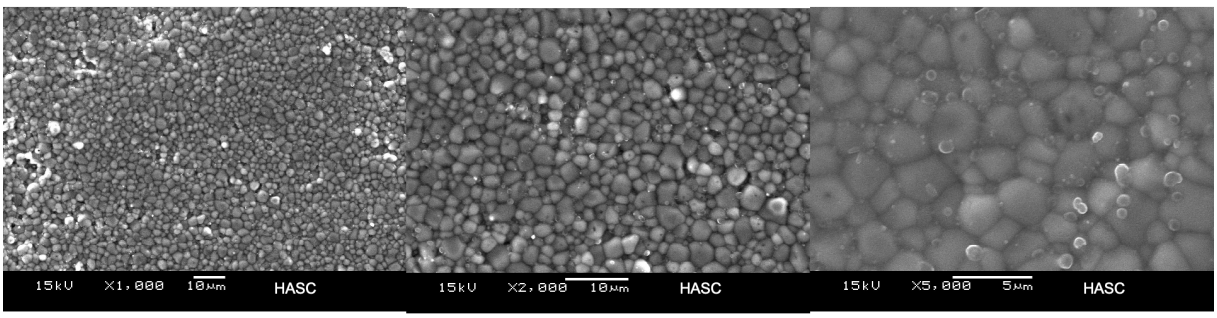

of binders and sintered by the conventional method
Source: Elaborated by the author

Figure 10- Fracture images (x1000, x2000 and x5000) of a hydroxyapatite specimen added with binders and sintered by the *2-step* method

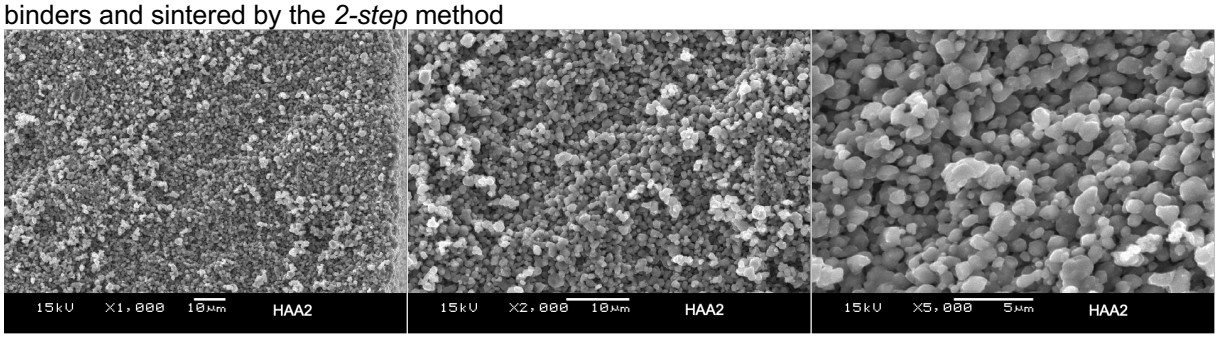

Source: Elaborated by the author

Figure 11- Fracture images (x1000, x2000 and x5000) of a hydroxyapatite specimen without addition of binders and sintered by the *2-step* method

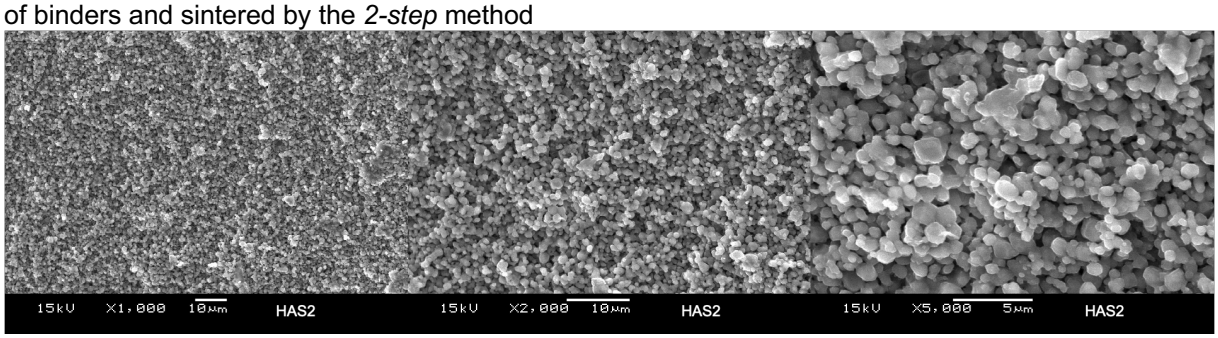

Source: Elaborated by the author

Figure 12- Fracture images (x1000, x2000 and x5000) of a hydroxyapatite specimen added with binders and sintered by the conventional method

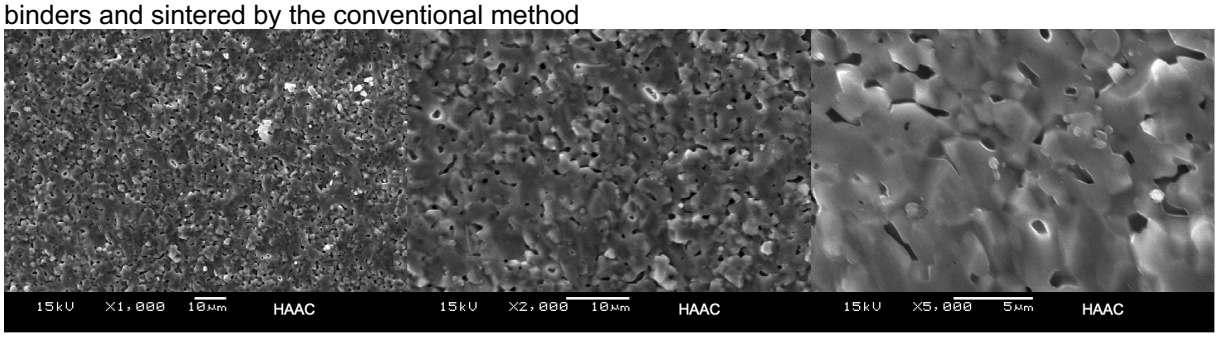

Source: Elaborated by the author

Figure 13- Fracture images (x1000, x2000 and x5000) of a hydroxyapatite specimen without addition of binders and sintered by the conventional method

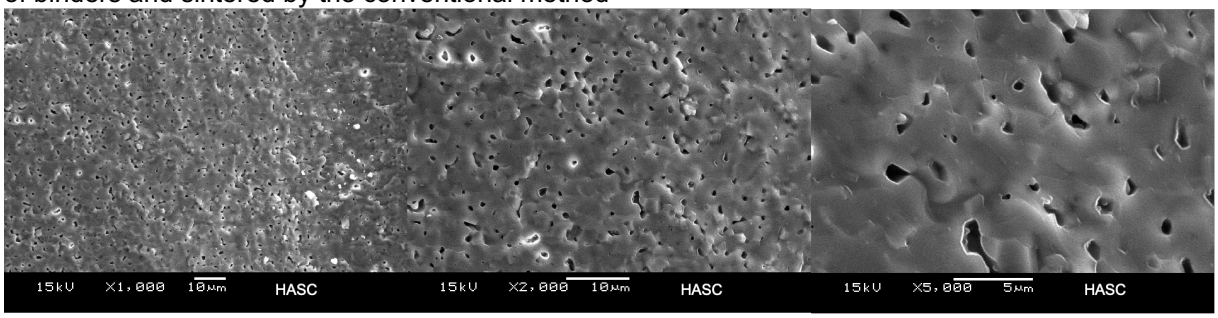

Source: Elaborated by the author

The results of Energy Scatter X-ray Spectroscopy showed in Figure 14 only the chemical elements expected for a hydroxyapatite sample, which allowed us to infer that there was no contamination of the samples by other elements.

Figure 14- Energy scattering X-ray spectra

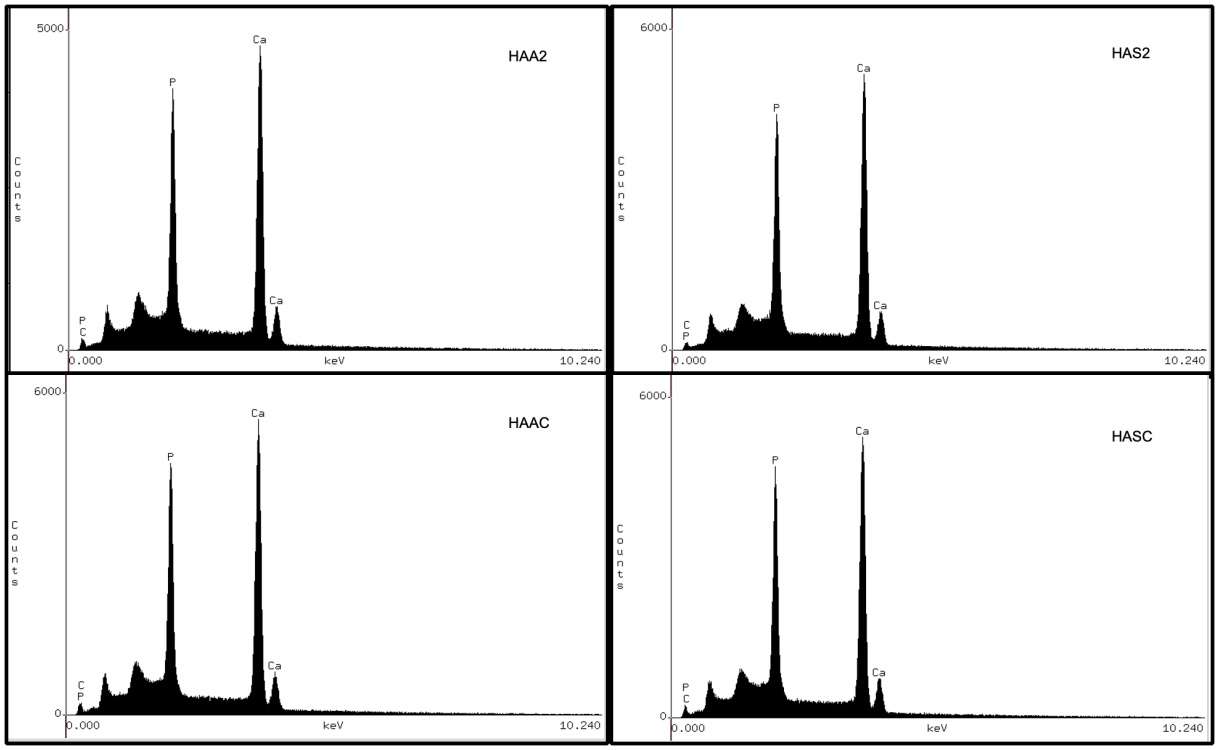

Source: Elaborated by the author

2.3.5. Density

Table 2 presents the p-values of the pairwise comparisons of the densities of the four groups. There was no statistically significant difference ($p = 0.252$) between groups HAA2 and HAS2, while all other intergroup comparisons were statistically different ($p < 0.05$).

The HASC group showed the best results (2.90, 2.93; 2.92$\frac{g}{cm^3}$) , reaching the highest density values, followed by HAAC (2.84, 2.86; 2.85 $\frac{g}{cm^3}$) and the groups HAS2 (2.07, 2.08; 2.08 $\frac{g}{cm^3}$) and HAA2 (2.06, 2.07; 2.07 $\frac{g}{cm^3}$), as can be seen in Table 3.

After calculating the values referring to the density relative to the median of the HASC group, it presented a value of 89.1%, followed by the HAAC group (86.9%) and HAS2 (64.4%) and HAA2 (63.1%).

Table 2- Comparison of density between groups

HASC	$\boldsymbol{p < 0,001}$	$\boldsymbol{p < 0,001}$	$\boldsymbol{p < 0,001}$	–
HAAC	$p < 0{,}001$	$p < 0{,}001$	–	–
HAS2	$p = 0.25$	–	–	–
HAA2	–	–	–	–
	HAA2	**HAS2**	**HAAC**	**HASC**

Source: Elaborated by the author

Table 3- Density of the evaluated groups

Material	Median	1st quartile	3rd quartile	p
HASC	2.92	2.90	2.93	0.74
HAAC	2.85	2.84	2.86	0.09
HAS2	2.08	2.07	2.08	0.22
HAA2	2.07	2.06	2.07	0.82

Source: Elaborated by the author

2.3.6. **Biaxial flexural fracture resistance**

The flexural strength data obtained from the surface bending are presented in Table 4. The results, as indicated in Table 5, showed a difference of statistical significance ($p < 0.05$) between the groups. The HASC group (98.0, 117.0; 109.0 MPa) presented the highest flexural strength, followed by HAAC (80.9, 98.9; 86.6 MPa), HAA2 (23.0, 26.8; 25.7 MPa) and HAS2 (18.7, 24.2; 20.3 MPa), respectively.

Table 4- Biaxial flexural fracture resistance of the groups

Material	Median	1st quartile	3rd quartile	p
HASC	109.0	98.0	117.0	0.73
HAAC	86.6	80.9	98.9	0.02
HAA2	25.7	23.0	26.8	0.24
HAS2	20.3	18.7	24.2	0.13

Source: Elaborated by the author

Table 5- Comparison of biaxial flexural fracture resistance between groups

HASC	$\boldsymbol{p}$ < 0.001	$\boldsymbol{p}$ < 0.001	$\boldsymbol{p}$ = 0.023	–
HAAC	p < 0.001	$p < 0.001$	–	–
HAS2	p = 0.042	–	–	–
HAA2	–	–	–	–
	HAA2	**HAS2**	**HAAC**	**HASC**

Source: Elaborated by the author

2.3.7. Modulus of elasticity

The HAAC ($106.10 \pm 8.01\ GPa$) and HASC ($105.17 \pm 14.65\ GPa$) groups presented equal values of modulus of elasticity, according to the margin of error of the Sonelastic® equipment (ATCP), followed by HAA2 ($38.89 \pm 4.72\ GPa$) and HAS2 ($34.07 \pm 2.20\ GPa$), also equivalent in the margin of error.

2.4. DISCUSSION

The similarity of hydroxyapatite with the mineral phase of bone tissue is the main impetus for the study and development of HA-dense ceramics. Therefore, to produce a dense ceramic, it is necessary to obtain, at the end of the sintering process, a product of adequate size, shape and properties. The shape and size are determined in the forming process, while the final properties of the product depend on several factors, such as the chemical composition of the material, its average grain size and the density of the ceramic at the end of sintering, making each step of the processing essential to guarantee the behaviour of the material (65,66).

In the DTA analysis for the hydroxyapatite sample with binders, the first peak, with a temperature around 125 °C, refers to an endothermic process attributed to the dehydration of the sample, that is, loss of water adsorbed on the surface of the material. This process was not observed in the sample without binding agents. The second peak, with a temperature in the range of 550 to 750 °C, refers to an exothermic process, which may be due to the decarboxylation of the samples, as reported by JOSCHEK et al. (67) (2000).

In all evaluated groups, the XRD spectra showed only the crystallographic peaks of HA. These characteristic spectra were also obtained in the work of Pires et al. (33) (2020). Evidencing that neither the presence of binders nor the different sintering methods produced alterations to the crystal structure of hydroxyapatite ceramics.

The non-interference of the evaluated factors (binders and sintering process) was also verified in the FTIR and EDS spectroscopic studies, since in the energy dispersion only the chemical elements expected for HA were found. And in the infrared, all materials maintained the characteristic bonds of HA, such as bands 1101, 1026, 633 and 560 cm^{-1} , referring to $(PO_4)^{3-}$, at 1650 cm^{-1} referring to H_2O, at 1545 cm^{-1} referring to the CO_2 and 2010 referring to $Ca^{2+} - CO$ (63,64).

The scanning electron microscopy images showed a higher number of pores in the ceramics submitted to *2-step* sintering when compared to those submitted to conventional sintering. A different result from what was reported by other researchers

who defined sintering in two stages without the use of high pressure, as a well-established low-cost method to obtain dense ceramics with restricted grain growth, managing to produce nanostructures in a simple and efficient way, including materials based on HA, using ovens used in conventional sintering (44–49).

However, although it is possible to observe, in the images of the *2-step* groups, small-sized grains, these samples showed an abundance of pores, which may be related to an incomplete sintering of the samples, given that it is possible to observe, both in the images surface and fracture region (Figures 6 – 13) the formation of necks between some grains, which indicates that the sample reached the second sintering stage, but possibly did not have enough energy to reach the third stage, where sintering process is completed (36).

The density results indicated that the ceramics submitted to *2-step* sintering, HAA2 and HAS2, did not differ significantly from each other and presented lower intensities, 2.07 g/cm^{-1} and 2.08 g/cm^{-1} , respectively, followed by the HAAC (2.85 g/cm^{-1}) and HASC (2.92 g/cm^{-1}) groups. The relative density values for each group are, respectively, 63.1%, 63.4%, 86.9% and 89.1%, considering 100% sintering, the value of 3.28 obtained in the pycnometry test. The relative density results for HA ceramics obtained by conventional sintering are in the range found in the literature, between 83 to 99% (44,68–72). However, those submitted to *2-step* sintering showed lower relative density than the values found by Lin et al. (44) (2012).

According to Rezaee, khoie, Liu (73) (2011), in order to better assess the flexural strength of materials with lower strength values, the most reliable test to perform is the biaxial flexural strength test using disk-shaped specimens. Of the groups evaluated, the HASC group (109.0 MPa) presented the highest flexural strength, followed by HAAC (86.6 MPa), HAA2 (25.7 MPa) and HAS2 (20.3 MPa), respectively.

The evaluated factors (binders and sintering) influenced the flexural strength of the evaluated ceramics. All groups differed significantly $p < 0.05$ among themselves and the group that showed the highest strength (109.0 MPa) was the one without binders and with conventional sintering. This resistance value is lower than that found by Pires et al. (33) (2020) (235.2 MPa) that used the same binders and conventional sintering parameters. However, in both studies, different methodologies were used for the drying of HA powders, which may explain the difference between the values found.

The HA ceramics from the groups subjected to conventional sintering showed elastic modulus values about three times higher than those reached by the groups submitted to *2-step* sintering. The values of Young's modulus of the HASC and HAAC groups are consistent with the values (80 - 110 GPa) found in the literature (57,74–76).

The low performance of the mechanical properties of ceramics subjected to *2-step* sintering can be explained by the parameters of temperature and time adopted. The defined temperatures were based on the model proposed by Lourenço (45), (2011), and were maximum temperature (T_{max}) of 950 °C and followed by a holding temperature (T_m) of 880 °C / 12 hours. These parameters differ from those used by Lin et al. (44) (2022), T_{max} = 1050 °C and T_m = 950 °C / 20 hours, which obtained better mechanical properties.

2.5. CONCLUSIONS

Under the applied experimental conditions, the hydroxyapatite ceramics subjected to conventional sintering showed better mechanical properties than those submitted to *2-step* sintering, based on the temperature and times chose.

The non-use of binders, in applications where it could be excluded, in the manufacture of HA ceramics proved to be favourable to the improvement of some mechanical properties.

Ceramics subjected to conventional sintering and without the addition of binding agents achieved the best results and managed to improve the mechanical properties of hydroxyapatite ceramic, inside of the experimental variations of this experiment.

Referências

REFERÊNCIAS

1. EMBRAPA. Brasil é o quarto maior produtor de grãos e o maior exportador de carne bovina do mundo, diz estudo - Portal Embrapa [Internet]. 2021 [cited 2022 May 24]. Available from: https://www.embrapa.br/busca-de-noticias/-/noticia/62619259/brasil-e-o-quarto-maior-produtor-de-graos-e-o-maior-exportador-de-carne-bovina-do-mundo-diz-estudo
2. Arvanitoyannis IS, Ladas D. Meat waste treatment methods and potential uses. International Journal of Food Science & Technology [Internet]. 2008 Mar 1 [cited 2022 Apr 24];43(3):543–59. Available from: https://onlinelibrary.wiley.com/doi/full/10.1111/j.1365-2621.2006.01492.x
3. Jayathilakan K, Sultana K, Radhakrishna K, Bawa AS. Utilization of byproducts and waste materials from meat, poultry and fish processing industries: a review. J Food Sci Technol [Internet]. 2012 Jun [cited 2022 Apr 24];49(3):278–93. Available from: https://pubmed.ncbi.nlm.nih.gov/23729848/
4. Yukalang N, Clarke B, Ross K. Solid Waste Management Solutions for a Rapidly Urbanizing Area in Thailand: Recommendations Based on Stakeholder Input. Int J Environ Res Public Health [Internet]. 2018 Jul 1 [cited 2022 Apr 24];15(7). Available from: https://pubmed.ncbi.nlm.nih.gov/29933621/
5. Shaikh MS, Zafar MS, Alnazzawi A, Javed F. Nanocrystalline hydroxyapatite in regeneration of periodontal intrabony defects: A systematic review and meta-analysis. Annals of Anatomy. 2022 Feb 1;240.
6. Hu YY, Rawal A, Schmidt-Rohr K. Strongly bound citrate stabilizes the apatite nanocrystals in bone. Proc Natl Acad Sci U S A. 2010 Dec 28;107(52):22425–9.
7. Batchelar DL, Davidson MTM, Dabrowski W, Cunningham IA. Bone-composition imaging using coherent-scatter computed tomography: assessing bone health beyond bone mineral density. Med Phys

[Internet]. 2006 [cited 2022 May 16];33(4):904–15. Available from: https://pubmed.ncbi.nlm.nih.gov/16696465/

8. Malmberg P, Nygren H. Methods for the analysis of the composition of bone tissue, with a focus on imaging mass spectrometry (TOF-SIMS). Proteomics [Internet]. 2008 Sep [cited 2022 May 16];8(18):3755–62. Available from: https://pubmed.ncbi.nlm.nih.gov/18780399/
9. Sato K. Mechanism of Hydroxyapatite Mineralization in Biological Systems (Review). Journal of the Ceramic Society of Japan. 2007;115(1338):124–30.
10. Sadat-Shojai M, Khorasani MT, Dinpanah-Khoshdargi E, Jamshidi A. Synthesis methods for nanosized hydroxyapatite with diverse structures. Vol. 9, Acta Biomaterialia. Elsevier Ltd; 2013. p. 7591–621.
11. Ibrahim M, Labaki M, Giraudon JM, Lamonier JF. Hydroxyapatite, a multifunctional material for air, water and soil pollution control: A review. Vol. 383, Journal of Hazardous Materials. Elsevier B.V.; 2020.
12. Paulo Espíndola Trani. Farinha dos ossos bovinos é opção a adubos químicos [Internet]. 2007 [cited 2022 Apr 24]. Available from: https://www.agrolink.com.br/noticias/farinha-dos-ossos-bovinos-e-opcao-a-adubos-quimicos_54958.html
13. Mondal S, Pal U, Dey A. Natural origin hydroxyapatite scaffold as potential bone tissue engineering substitute. Ceramics International. 2016 Dec 1;42(16):18338–46.
14. Sopyan I, Mel M, Ramesh S, Khalid KA. Porous hydroxyapatite for artificial bone applications. Science and Technology of Advanced Materials. 2007 Jan;8(1–2):116–23.
15. Ioku K. Tailored bioceramics of calcium phosphates for regenerative medicine. Journal of the Ceramic Society of Japan. 2010 Sep 1;118(1381):775–83.
16. Surmeneva MA, Mukhametkaliyev TM, Khakbaz H, Surmenev RA, Bobby Kannan M. Ultrathin film coating of hydroxyapatite (HA) on a magnesium–calcium alloy using RF magnetron sputtering for bioimplant applications. Materials Letters. 2015 Aug 1;152:280–2.
17. Palazzo B, Sidoti MC, Roveri N, Tampieri A, Sandri M, Bertolazzi L, et al. Controlled drug delivery from porous hydroxyapatite grafts: An

experimental and theoretical approach. Materials Science and Engineering C [Internet]. 2005 Apr 28 [cited 2022 Apr 24];25(2):207–13. Available from: https://moh-it.pure.elsevier.com/en/publications/controlled-drug-delivery-from-porous-hydroxyapatite-grafts-an-exp

18. Weerasuriya DRK, Wijesinghe WPSL, Rajapakse RMG. Encapsulation of anticancer drug copper bis(8-hydroxyquinoline) in hydroxyapatite for pH-sensitive targeted delivery and slow release. Mater Sci Eng C Mater Biol Appl [Internet]. 2017 Feb 1 [cited 2022 Apr 24];71:206–13. Available from: https://pubmed.ncbi.nlm.nih.gov/27987700/
19. Son JS, Appleford M, Ong JL, Wenke JC, Kim JM, Choi SH, et al. Porous hydroxyapatite scaffold with three-dimensional localized drug delivery system using biodegradable microspheres. J Control Release [Internet]. 2011 Jul 30 [cited 2022 Apr 24];153(2):133–40. Available from: https://pubmed.ncbi.nlm.nih.gov/21420453/
20. Cummings LJ, Snyder MA, Brisack K. Protein chromatography on hydroxyapatite columns. Methods Enzymol [Internet]. 2009 [cited 2022 Apr 24];463(C):387–404. Available from: https://pubmed.ncbi.nlm.nih.gov/19892184/
21. Kalita SJ, Rokusek D, Bose S, Hosick HL, Bandyopadhyay A. Effects of MgO-CaO-P2O5-Na2O-based additives on mechanical and biological properties of hydroxyapatite. J Biomed Mater Res A [Internet]. 2004 Oct 1 [cited 2022 Apr 24];71(1):35–44. Available from: https://pubmed.ncbi.nlm.nih.gov/15368252/
22. Kweon HY, Lee SW, Hahn BD, Lee YC, Kim SG. Hydroxyapatite and silk combination-coated dental implants result in superior bone formation in the peri-implant area compared with hydroxyapatite and collagen combination-coated implants. J Oral Maxillofac Surg [Internet]. 2014 [cited 2022 Apr 24];72(10):1928–36. Available from: https://pubmed.ncbi.nlm.nih.gov/25234528/
23. Hung KY, Lo SC, Shih CS, Yang YC, Feng HP, Lin YC. Titanium surface modified by hydroxyapatite coating for dental implants. Surface and Coatings Technology [Internet]. 2013 Sep 25 [cited 2022 Apr 24];C(231):337–45. Available from:

https://www.infona.pl//resource/bwmeta1.element.elsevier-024bd928-efe0-3ba9-be24-6176847e9a3f

24. Pires LA, de Azevedo Silva LJ, Ferrairo BM, Erbereli R, Lovo JFP, Ponce Gomes O, et al. Effects of ZnO/TiO2 nanoparticle and TiO2 nanotube additions to dense polycrystalline hydroxyapatite bioceramic from bovine bones. Dent Mater [Internet]. 2020;36(2):e38–46. Available from: https://www.embase.com/search/results?subaction=viewrecord&id=L630098629&from=export
25. Araújo PPP, Costa LP. Impactos ambientais nas atividades de abate de bovinos: um estudo no matadouro público municipal de Caicó-RN. Holos. 2014;1–20.
26. Jabbour ABL de S, Jabbour CJC. Gestão ambiental nas organizações : fundamentos e tendências. Atlas. 2013;1:1–112.
27. Mattar EPL, Frade Júnior EF, de Oliveira E. Caracterização físico-química de cinza de osso bovino para avaliação do seu potencial uso agrícola. Pesquisa Agropecuária Tropical [Internet]. 2014 [cited 2022 Apr 24];44(1):65–70. Available from: http://www.scielo.br/j/pat/a/GVwMQ4LQpQtJqdknfXLMQWz/?lang=pt
28. Szabó-Junior AM. Educação ambiental e gestão de resíduos. Rideel. 3rd ed. 2010;1–118.
29. Bohner M. Calcium orthophosphates in medicine: from ceramics to calcium phosphate cements. Injury [Internet]. 2000 [cited 2022 May 16];31 Suppl 4(SUPPL. 4). Available from: https://pubmed.ncbi.nlm.nih.gov/11270080/
30. Vallet-Regí M, González-Calbet JM. Calcium phosphates as substitution of bone tissues. Progress in Solid State Chemistry [Internet]. 2004 [cited 2022 May 15];32(1–2):1–31. Available from: www.elsevier.nl/locate/pssc
31. Galdino AD. Produção e Caracterização de Arcabouços Porosos de compósitos Hidroxiapatita-Titânia (HA-TiO2) para Uso em Engenharia Tecidual Óssea. [Campinas]: Unicamp; 2011.
32. C L, W W, W S, T C, L H, Z C. Evaluation of the biocompatibility of a nonceramic hydroxyapatite. J Endod [Internet]. 1997 [cited 2022 May 16];23(8):490–3. Available from: https://pubmed.ncbi.nlm.nih.gov/9587317/

33. Pires LA, de Azevedo Silva LJ, Ferrairo BM, Erbereli R, Lovo JFP, Ponce Gomes O, et al. Effects of ZnO/TiO2 nanoparticle and TiO2 nanotube additions to dense polycrystalline hydroxyapatite bioceramic from bovine bones. Dent Mater [Internet]. 2020;36(2):e38–46. Available from: https://www.embase.com/search/results?subaction=viewrecord&id=L630098629&from=export
34. Rey C, Combes C, Drouet C, Sfihi H, Barroug A, Physico-Chemical AB, et al. Physico-chemical properties of nanocrystalline apatites: Implications for biominerals and biomaterials Open Archive Toulouse Archive Ouverte (OATAO) Physico-chemical properties of nanocrystalline apatites: Implications for biominerals and biomaterials. 2007;27(2):198–205.
35. Elliot J. C. Structure and Chemistry of the Apatites and Other Calcium Orthophosphates - J.C. Elliott - Google Libros. 1994 [cited 2022 Apr 24];63–230. Available from: https://books.google.com.mx/books?hl=es&lr=&id=dksXBQAAQBAJ&oi=fnd&pg=PP1&dq=Structure+and+chemistry+of+the+apatites+and+other+calcium+orthophosphates.+Studies+in+inorganic+chemistry&ots=xqNFMG_Pt2&sig=lSkXSk5wAus8VTnsyftTLZO_PMc#v=onepage&q=Structure and
36. Prakasam M, Locs J, Salma-Ancane K, Loca D, Largeteau A, Berzina-Cimdina L. Fabrication, Properties and Applications of Dense Hydroxyapatite: A Review. Journal of Functional Biomaterials 2015, Vol 6, Pages 1099-1140 [Internet]. 2015 Dec 21 [cited 2022 May 16];6(4):1099–140. Available from: https://www.mdpi.com/2079-4983/6/4/1099/htm
37. M N Rahaman. Ceramic Processing and Sintering: 1 [Internet]. 2nd ed. Part III Materials Science, University of Cambridge. 2003 [cited 2022 May 19]. 1–875 p. Available from: https://www.vle.cam.ac.uk/pluginfile.php/6769581/mod_resource/content/3/S5 Handout - FINAL.pdf
38. Barraclough KG, Loni A, Caffull E, Canham LT. Cold compaction of silicon powders without a binding agent. Materials Letters. 2007 Jan;61(2):485–7.

39. Mosquim V, Ferrairo BM, Vertuan M, Magdalena AG, Fortulan CA, Lisboa-Filho PN, et al. Structural, chemical and optical characterizations of an experimental SiO2–Y-TZP ceramic produced by the uniaxial/isostatic pressing technique. Journal of the Mechanical Behavior of Biomedical Materials. 2020 Jun 1;106.
40. Canillas M, Pena P, de Aza AH, Rodríguez MA. Calcium phosphates for biomedical applications. Boletín de la Sociedad Española de Cerámica y Vidrio. 2017 May 1;56(3):91–112.
41. Prokopiev O, Sevostianov I. Dependence of the mechanical properties of sintered hydroxyapatite on the sintering temperature. Materials Science and Engineering: A. 2006 Sep 15;431(1–2):218–27.
42. Obada DO, Dauda ET, Abifarin JK, Dodoo-Arhin D, Bansod ND. Mechanical properties of natural hydroxyapatite using low cold compaction pressure: Effect of sintering temperature. Materials Chemistry and Physics. 2020 Jan 1;239.
43. Borum L, Wilson OC. Surface modification of hydroxyapatite. Part II. Silica. Biomaterials [Internet]. 2003 [cited 2022 May 16];24(21):3681–8. Available from: https://pubmed.ncbi.nlm.nih.gov/12818539/
44. Lin K, Chen L, Chang J. Fabrication of Dense Hydroxyapatite Nanobioceramics with Enhanced Mechanical Properties via Two-Step Sintering Process. International Journal of Applied Ceramic Technology [Internet]. 2012 May 1 [cited 2022 May 18];9(3):479–85. Available from: https://onlinelibrary.wiley.com/doi/full/10.1111/j.1744-7402.2011.02654.x
45. Lourenço MA, Cunto GG, Figueiredo FM, Frade JR. Model of two-step sintering conditions for yttria-substituted zirconia powders. Materials Chemistry and Physics. 2011 Mar 15;126(1–2):262–71.
46. Wang XH, Chen PL, Chen IW. Two-Step Sintering of Ceramics with Constant Grain-Size, I. Y Two-Step Sintering of Ceramics with Constant Grain-Size, I. Y 2 2 O O 3 3. 2006 [cited 2022 May 24]; Available from: https://repository.upenn.edu/mse_papers
47. Dong Y, Chen IW. Mobility transition at grain boundaries in two-step sintered 8 mol% yttria-stabilized zirconia. Journal of the American Ceramic Society [Internet]. 2018 May 1 [cited 2022 May

24];101(5):1857–69. Available from: https://onlinelibrary.wiley.com/doi/full/10.1111/jace.15362

48. Wei C, Gremillard L. Towards the prediction of hydrothermal ageing of 3Y-TZP bioceramics from processing parameters. Acta Materialia. 2018 Feb 1;144:245–56.
49. Villas-Boas LA, Goulart CA, Kiminami RHGA, de Souza DPF. A case study of ceramic processing: Microstructural development and electrical properties of Ce0.8Gd0.2O1.9. Ceramics International. 2020 Jun 1;46(8):12318–28.
50. Berkun M, Aras E, Anılan T. Solid waste management practices in Turkey. Journal of Material Cycles and Waste Management [Internet]. 2011 Sep 30 [cited 2022 May 24];13(4):305–13. Available from: https://link.springer.com/article/10.1007/s10163-011-0028-7
51. Fang Z, Feng Q, Tan R. In-situ grown hydroxyapatite whiskers reinforced porous HA bioceramic. Ceramics International. 2013 Dec 1;39(8):8847–52.
52. Jäger M, Jennissen HP, Dittrich F, Fischer A, Köhling HL. Antimicrobial and Osseointegration Properties of Nanostructured Titanium Orthopaedic Implants. Materials 2017, Vol 10, Page 1302 [Internet]. 2017 Nov 13 [cited 2022 May 24];10(11):1302. Available from: https://www.mdpi.com/1996-1944/10/11/1302/htm
53. Gamelas JAF, Martins AG. Surface properties of carbonated and non-carbonated hydroxyapatites obtained after bone calcination at different temperatures. Colloids and Surfaces A: Physicochemical and Engineering Aspects. 2015 Aug 5;478:62–70.
54. Bouslama N, ben Ayed F, Bouaziz J. Effect of fluorapatite additive on densification and mechanical properties of tricalcium phosphate. Journal of the Mechanical Behavior of Biomedical Materials. 2010 Jan 1;3(1):2–13.
55. Ramesh S, Tan CY, Tolouei R, Amiriyan M, Purbolaksono J, Sopyan I, et al. Sintering behavior of hydroxyapatite prepared from different routes. Materials & Design. 2012 Feb 1;34:148–54.
56. Sebdani MM, Fathi MH. Preparation and characterization of hydroxyapatite–forsterite–bioactive glass nanocomposite coatings for

biomedical applications. Ceramics International. 2012 Mar 1;38(2):1325–30.

57. Meira CR. Processamento de hidroxiapatita bovina associada com prototipagem rápida visando implantes ósseos. [São Carlos]: Universidade de São Paulo; 2014.
58. American Society for Testing and Materials. ASTM, Standard Specification For Composition Of Hydroxylapatite For Surgical Implants - F1185-14(2014). 2014.
59. International Standards Organization. ISO 6872, Dentistry – Ceramic Materials. Switzerland; 2015.
60. Alarcon RT, Gaglieri C, Caires FJ, Magdalena AG, de Castro RAE, Bannach G. Thermoanalytical study of sweetener myo-inositol: α and β polymorphs. Scopus [Internet]. 2017 Dec 15 [cited 2022 Apr 24];237:1149–54. Available from: https://repositorio.unesp.br/handle/11449/178953
61. Associação Brasileira de Normas Técnicas. ABNT NBR 16661 - Materiais refratários densos conformados - Determinação do volume aparente, volume aparente da parte sólida, densidade de massa aparente, densidade aparente da parte sólida, porosidade aparente e absorção. Brazil: Associação Brasileira de Normas Técnicas; 2017.
62. American Society for Testing and Materials. ASTM, Standard Test Method for Dynamic Young's Modulus, Shear Modulus, and Poisson's Ratio by Impulse Excitation of Vibratio - E 1876-15. 2015.
63. Pekounov Y, Chakarova K, Hadjiivanov K. Surface acidity of calcium phosphate and calcium hydroxyapatite: FTIR spectroscopic study of low-temperature CO adsorption. Materials Science and Engineering: C. 2009 May 5;29(4):1178–81.
64. Veiga A, Castro F, Reis C, Sousa A, Oliveira AL, Rocha F. Hydroxyapatite/sericin composites: A simple synthesis route under near-physiological conditions of temperature and pH and preliminary study of the effect of sericin on the biomineralization process. Materials Science and Engineering: C. 2020 Mar 1;108:110400.
65. Binner J. Advanced ceramic processing and technology. Noyes Publications; 1990. 1–415 p.

66. Pires LA. Avaliação estrutural, morfológica e mecânica de cerâmica densa de hidroxiapatita bovina reforçada com nanotubos de TiO2 e nanopartículas de ZnO e TiO2 [Internet]. [Bauru]: Universidade de São Paulo; 2019 [cited 2022 May 24]. Available from: https://www.teses.usp.br/teses/disponiveis/25/25148/tde-05102021-082852/

67. Joschek S, Nies B, Krotz R, Göpferich A. Chemical and physicochemical characterization of porous hydroxyapatite ceramics made of natural bone. Biomaterials. 2000 Aug 1;21(16):1645–58.

68. Chen B, Zhang T, Zhang J, Lin Q, Jiang D. Microstructure and mechanical properties of hydroxyapatite obtained by gel-casting process. Ceramics International. 2008 Mar 1;34(2):359–64.

69. Hoepfner TP, Case ED. The influence of the microstructure on the hardness of sintered hydroxyapatite. Ceramics International. 2003 Jan 1;29(6):699–706.

70. Thangamani N, Chinnakali K, Gnanam FD. The effect of powder processing on densification, microstructure and mechanical properties of hydroxyapatite. Ceramics International. 2002 Jan 1;28(4):355–62.

71. Banerjee A, Bandyopadhyay A, Bose S. Hydroxyapatite nanopowders: Synthesis, densification and cell–materials interaction. Materials Science and Engineering: C. 2007 May 16;27(4):729–35.

72. Tancred DC, Carr AJ, McCormack BAO. The sintering and mechanical behavior of hydroxyapatite with bioglass additions. J Mater Sci Mater Med [Internet]. 2001 [cited 2022 May 24];12(1):81–93. Available from: https://pubmed.ncbi.nlm.nih.gov/15348381/

73. Rezaee M, Mousavi Khoie SM, Liu KH. The role of brookite in mechanical activation of anatase-to-rutile transformation of nanocrystalline TiO2: An XRD and Raman spectroscopy investigation. CrystEngComm [Internet]. 2011 Jul 27 [cited 2022 May 24];13(16):5055–61. Available from: https://pubs.rsc.org/en/content/articlehtml/2011/ce/c1ce05185g

74. Suchanek W, Yoshimura M. Processing and properties of hydroxyapatite-based biomaterials for use as hard tissue replacement implants. Journal of Materials Research [Internet]. 1998 [cited 2022 May 24];13(1):94–117. Available from: https://www.cambridge.org/core/journals/journal-of-materials-research/article/processing-and-properties-of-hydroxyapatitebased-biomaterials-for-use-as-hard-tissue-replacement-implants/928F0FB7396B1A7A92FA34FED1544F2B
75. PEREIRA MM, VASCONCELOS WL, ZAVAGLIA CAC. Materiais cerâmicos –ciência e aplicação como biomateriais: fundamentos e aplicações. Rio de Janeiro: Cultura Médica; 2006. 61–81 p.
76. KANAZAWA T. Inorganic phosphate materials. . 2nd ed. Tokyo: Kodansha; 1989. 1–288 p.